

Aircraft Ditching Impact Loads and Floatation Analysis

H. Climent*, J.T. Viana*, J. Espinosa de los Monteros*, F. Sánchez Iglesias* and L. González Fernández**

**Aeroelasticity & Structural Dynamics Department*

Airbus Defence and Space. Military Aircraft.

Hector.climent-manez@airbus.com

***ALTRAN innovación S.L.*

Lucia.gonzalezfernandez@altran.com

Abstract

Ditching is an emergency condition that ends with a controlled impact of the aircraft against water. Ditching analysis has four phases: aircraft conditions before impact; structural response during impact; sliding phase and subsequent floatation. The paper focuses in two of these phases, impact and floatation extensively showing how these two problems are solved in industry. In particular the paper compares three numerical ditching loads methodologies selecting the most suitable. Significant level of test validation using EU funded research program SMAES is shown. The paper ends with conclusions and proposals for further research in ditching.

1. Introduction

January 15th 2009 was a cold winter day in New York City. At 15:25 in La Guardia airport, Chesley “Sully” Sullenberger released the breaks of the Airbus A320 he was piloting bounded to Charlotte (NC). Just 208 seconds later he landed in the chilly waters of the Hudson River. All, crew and passengers up to a tally of 155, survived the ditching that day.

Ditching is a planned aircraft event that ends with a controlled emergency landing in water. Four main phases may be considered in a ditching event:

- **Approach:** Characterized by aircraft/environment conditions before impact.
- **Impact:** Structural response during the impact (fluid-structure interaction).
- **Landing:** Subsequent motion of the aircraft until stoppage.
- **Floatation:** evacuation of passengers and crew.

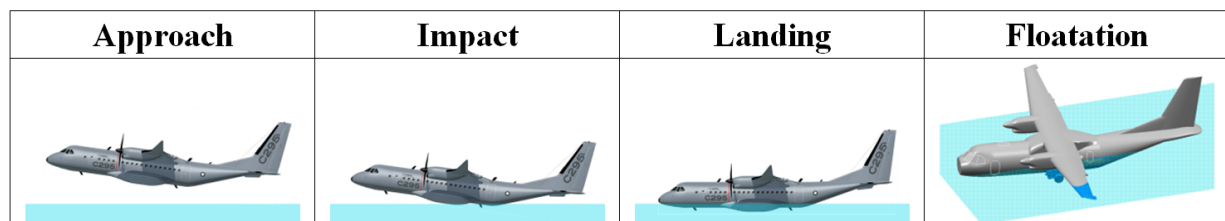


Figure 1: The Four Ditching Phases

This scenario is reflected in the Airworthiness Regulations that requires the aircraft manufacturer to take all necessary measures to minimize risk during ditching to allow the crew and passengers to evacuate the cabin safely. At Airbus DS Military Aircraft Structural Dynamics department ditching loads has been a topic of continuous research for more than 13 years [1-15]. This interest is also shared by universities, research laboratories and industrial partners that have gathered together in a recent European funded research project: SMAES (Smart Aircraft in Emergency Situation, 2011-1014).

SMAES devoted part of its activities to perform experimental ditching test of flat plates with different stiffness, material (metallic, composite), curvature, impact speeds and pitch angles. References [16-18] illustrate the SMAES results. SMAES tests were performed at the Italian CNR-INM Institute of Marine Engineering in Rome. The present paper focuses in two of the ditching phases: impact and floatation phases.

- **Impact phase:** loads generated during this phase could potentially break parts of bottom part of the aircraft fuselage jeopardizing subsequent evacuation. Current computer resources and enhancements of finite element technique allow addressing the numerical simulation of the impact phase using several methodologies and select the most suitable after benchmark with SMAES test results.
- **Floatation phase:** Once the aircraft has reached to a rest a new phase starts: floatation with the aim to demonstrate that there is enough floatation time to allow safe evacuation of all passengers. The paper describes a numerical approach to tackle this phase in calm and rough waters.

2. Ditching Impact Phase

2.1 General considerations in the aircraft ditching impact phase

During the fraction of a second of the ditching impact phase, large hydrodynamic pressures develop at the interface between the structure and the fluid which in turn may generate damages leading to rupture and cracks on the bottom part of the aircraft fuselage, a potential source of water ingress that could compromise subsequent safe evacuation. Strategy for justification of aircraft structure in the ditching scenario has three subtasks:

- 1) Generate an explicit Finite Element Method (FEM) model of the structure
- 2) Determine the load excitation during a ditching event
- 3) Obtain the structural response of the aircraft model to the ditching excitation

2.2 Generation of the explicit Finite Element Method model of the structure

The aircraft is modelled using the explicit Finite Element Method (FEM) technique, suitable to simulate any impact scenario and ditching in particular. Starting from the Global FEM model of the structure, the bottom part of the fuselage where the ditching impact will take place is extracted and the mesh of this part is significantly refined. Figure 2 illustrates this process and Figure 3 shows a zoom of the refined zone to illustrate the mesh size.

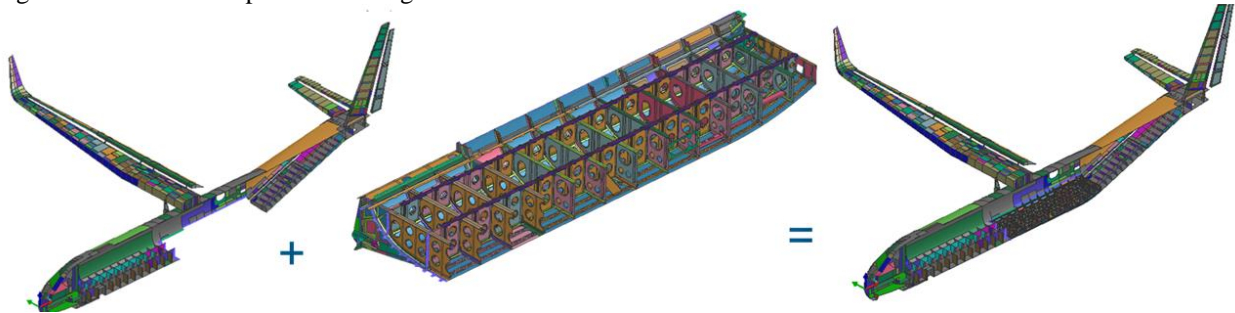


Figure 2. Global FEM model + Detailed bottom fuselage model = Integrated model for ditching calculations.

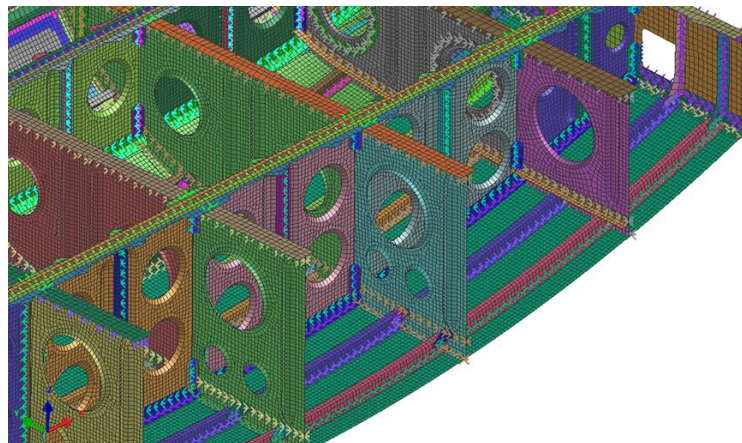


Figure 3. Zoom of the detailed bottom fuselage model to illustrate mesh size.

2.3 Determine the loads excitation during a ditching event

The determination of the loads that apply to the aircraft in a ditching scenario has been the core of significant research in recent years at Airbus DS Military Aircraft [1-15]. Among the various techniques explored, four will be presented in this paper:

- Experimental
- Synthetic Pressures (Analytical expressions that match experimental results)
- Smoothed Particle Hydrodynamics (SPH)
- Computational Fluid Dynamics (CFD)

2.3.1 Experimental Ditching Loads

The SMAES ditching tests are set of guided impact tests of panels against water at horizontal speeds representative of aircraft at landing condition. The objective was to measure the pressures acting on the panel and the structural deformation during the impact. To obtain a complete database, relevant parameters were varied during the test:

- Horizontal speed (30m/s, 40m/s, 50m/s) & Pitch angle at impact (4°, 6°, 10°)
- Panel curvature (flat, concave, convex) & Panel stiffness (rigid, flexible, very flexible)
- Panel material (Aluminium / Composite)

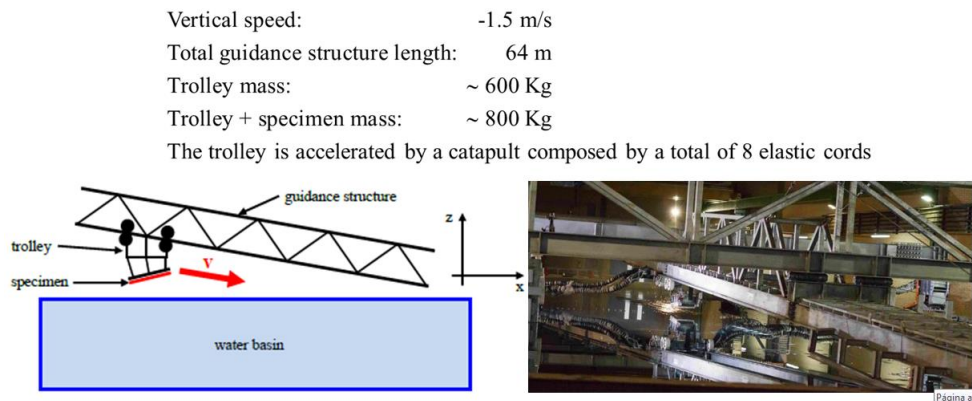


Figure 4. Sketch of the SMAES guided ditching test setup

The instrumentation of the guided ditching tests was very complete:

- 14 pressure transducers distributed in 18 possible different locations
- 8 strain gauges – two directions (16 channels)
- Velocity (1 channel)
- 2 biaxial and 2 single axis accelerometers on the panels (6 channels)
- 6 load cells to measure forces from the panel to the trolley (4 channels)

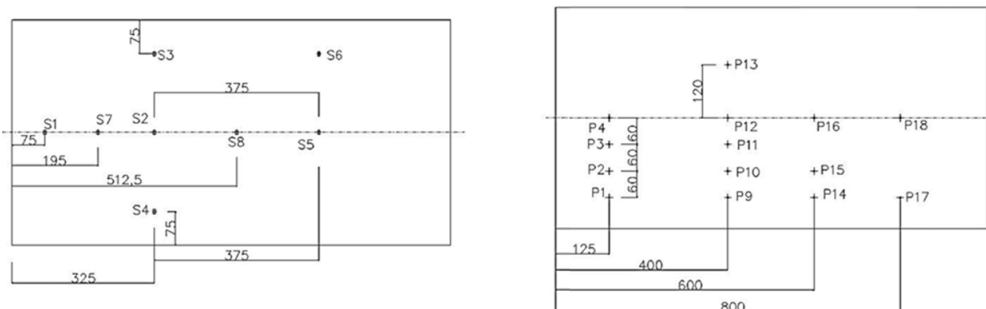


Figure 5. Schematic sketch of the SMAES strain gauges (left) and pressure transducers (right)

The SMAES program has allowed the determination of a very large data base of ditching pressures that could be used directly or to validate numerical tools. Next section will show three of these numerical techniques.

2.3.2 Synthetic Ditching Pressures

In a general way, the pressure time history can be expressed as a function of the (x,y) position in the panel and the initial conditions described in figure 6 (left). In light of the SMAES test results, the expression (1) plotted in figure 6 (right) seems appropriate to approximate analytically the pressure time histories obtained experimentally for a flat quasi-rigid panel ditching.

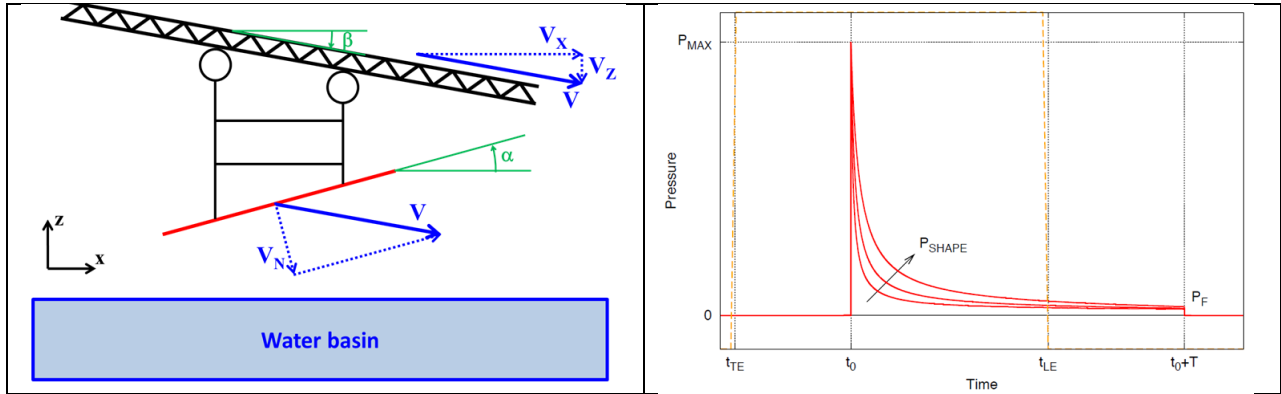


Figure 6: Initial ditching conditions sketch (left). Analytical approximation for the pressure time histories. (Right)

$$P(V_x, V_z, \alpha, x, t) = \begin{cases} P_F + \frac{P_{SHAPE}}{\tan\left[\frac{t-t_0}{T} \frac{\pi}{2} + \arctan\left(\frac{P_{SHAPE}}{P_{MAX} - P_F}\right)\right]} & , t_0 \leq t \leq t_0 + T \\ 0 & , t < t_0 \text{ \& } t > t_0 + T \end{cases} \quad (1)$$

Where:

| | |
|---|---|
| V_x, V_z, α | are the initial ditching conditions: horizontal speed, vertical speed and pitch angle |
| (x, y) | are the panel coordinates, with the origin in the central point of the trailing edge, x positive towards the direction of motion and y positive to port |
| t | is the time |
| $t_0 \equiv t_0(V_z, \alpha, x)$ | is the time instant for which $P = P_{MAX}$ |
| $P_{MAX} \equiv P_{MAX}(V_x, V_z, \alpha, x)$ | is the peak value of the pressure time history |
| $P_{SHAPE} \equiv P_{SHAPE}(V_x, V_z, \alpha, x)$ | is a shape factor that determines the decay rate of the pressure time history |
| $P_F \equiv P_F(V_x, V_z, \alpha, x)$ | is the final pressure value at $t = T + t_0$ |
| $T \equiv T(V_z, \alpha)$ | is an arbitrary but sufficiently large time as to make sure that the pressure time history has become almost flat |

2.3.3 Ditching Simulation Using Smoothed Particles Hydrodynamic Technique

The Smoothed Particle Hydrodynamics (SPH) is a grid-less computational technique where each SPH particle represents an interpolation point. Particles interact based on a weighted summation of their properties within a zone of influence controlled by the smoothing length. This technique has been widely used in Airbus DS Military Aircraft with the ©ESI Virtual Performance Solution (former PAM-CRASH) software [19].

SPH technique has been a very powerful tool in numerical simulation of impacts of aeronautical structures. The capacity of the **SPH** to properly handle very large deformations without exhibiting numerical instabilities has made them **the ideal way of modelling impactors** (bird, ice, stones, tyre fragments, debris...). The **SPH technique** is identified as one of the **key contributors** of the success of numerical simulations in aero structures. Past experience in Airbus DS Military Aircraft shows that, when the most important effect is the inertia effect, the SPH technique is the most suitable candidate to model the impactor.

Would the SPH technique be also a suitable candidate to model the sea in a ditching scenario? In fact, promising results have been obtained for helicopter ditching simulation [1]. Could these promising results in helicopters be extended to aircraft ditching with significant horizontal speed? To try to answer this question, the SMAES plate explicit FEM model has been considered in combination of a SPH sea. Figure 7 shows this simulation in which the plate has been launched on an SPH sea. Table 1 indicates the computer cost of these runs.

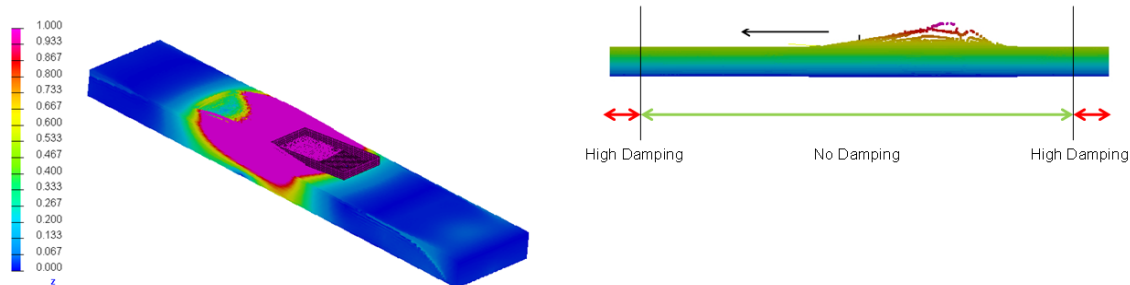


Figure 7: Numerical simulation of flat plate ditching against an SPH sea.

Table 1: CPU time of SPH ditching calculations (using [19] SPH implementation)

| | No. of SPH Particles | SPH size (spacing) | CPU Time (20 processors) |
|------------------------------------|----------------------|--------------------|--------------------------|
| Rigid Plate 1m x 0.5m | 0.4 Millions | 16 mm | 6 hours |
| Flexible Plate 1m x 0.5 m | 10 Millions | 5 mm | 1 week |
| Flexible Full Aircraft (estimated) | 250 Millions | Variable [5-16 mm] | 25 weeks |

2.3.4 Ditching Simulation Using Computational Fluid Dynamics

Taking the rigid flat plate of the SMAES as the simulated case of study, the first attempt was to simulate a 2D version in CFD and then compare the obtained pressures with the SMAES test in the plane of symmetry. The code used is ANSYS Fluent, versions 18.0 and 19.2. Table 2 shows the computer cost of these simulations.

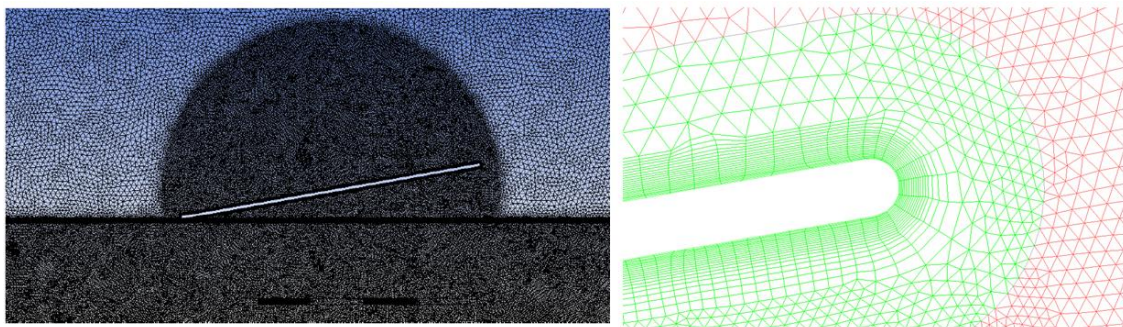


Figure 8 (Left) SMAES guided ditching test model implemented in ANSYS Fluent (2D). (Right) CFD Mesh

Table 2: CPU time of CFD ditching calculations

| | CPU Time (32 Processors) | Scalability (128 processors) |
|---------------------------------------|--------------------------|------------------------------|
| 2D Rigid Plate 1m x 0.5m | 4 days | No scalable |
| 3D Rigid Plate 1m x 0.5 m (estimated) | 40 days | ⇒ 10 days |
| Full Aircraft (estimated) | | 1 year? |

2.3.5 Comparison among experimental (SMAES) and three numerical methodologies (synthetic, SPH and CFD)

Figure 9 shows the comparison of the experimental results with the numerical methodologies.

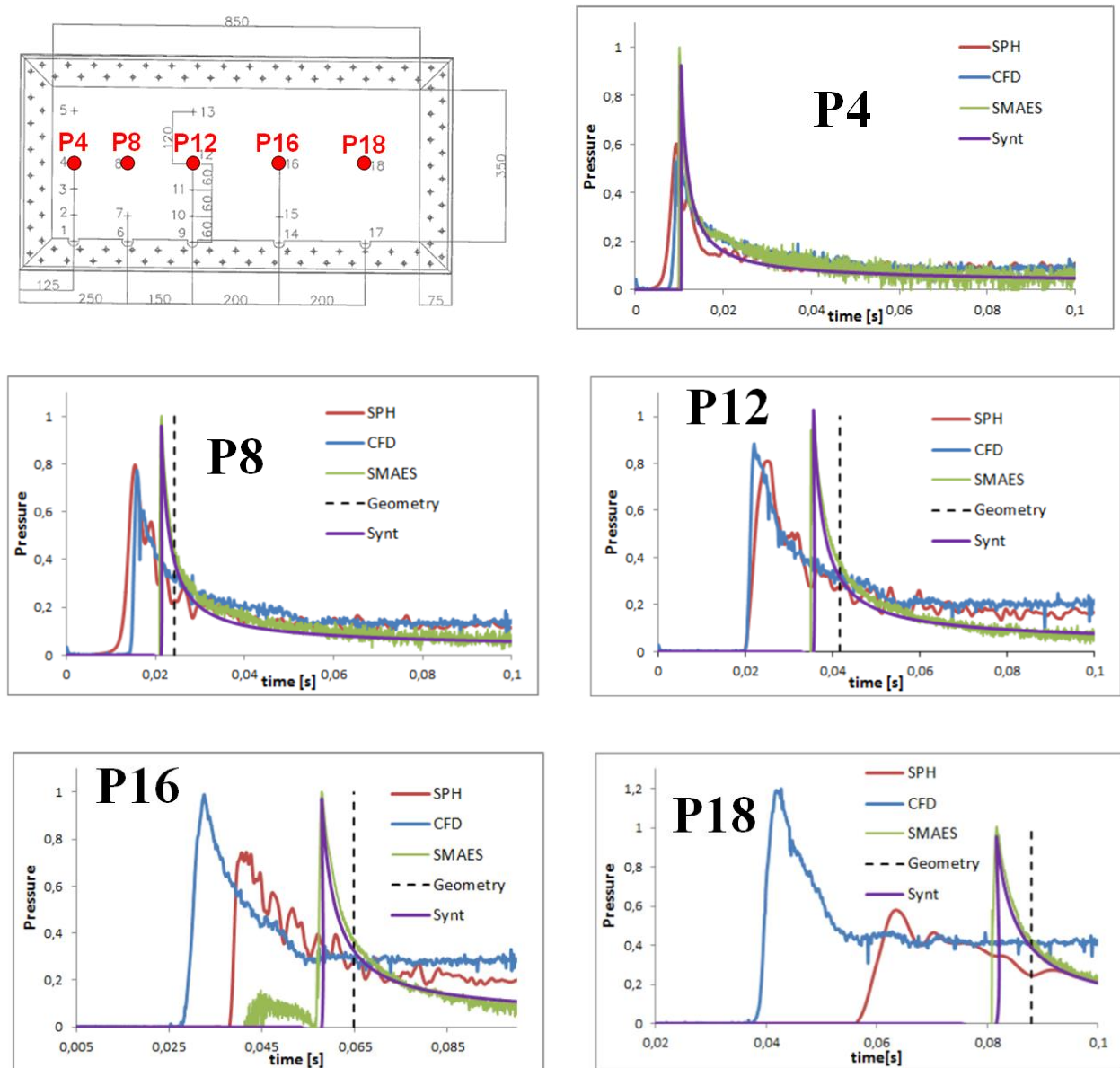


Figure 9. Comparison of different normalized ditching pressures numerical simulation methodologies with test results ($V_x=40$ m/s, pitch 10 degrees)

Comments from this comparison:

- The synthetic pressures provide –by construction–the best match of ditching test pressures in all the five gauges, in peak values, shapes and timing.
- The results obtained with Fluent (CFD) are very similar to the ones obtained with SPH for the three first gauges (P4, P8 and P12) but both methods, CFD and SPH, tend to underestimate the peak pressure, when compared with the experimental results in these first 3 gauges.
- CFD pressure results have a tendency to increase peak values and shapes when moving along the plate (for larger X values). This peak values trend is exactly the opposite trend measured in SMAES test results. In

addition, this CFD trend makes the prediction for probe P16 reasonable but for P18 very conservative. Both SPH and CFD tend to depart from experimental results in these two gauges.

- A shift of the time history appears in the experimental results due to the stream of water that rises towards the plate leading edge, when comparing SMAES test results with geometric line. SPH and CFD computational approaches predict the pressure peak earlier, being this time gap higher for the ANSYS Fluent simulations (especially for the last probes). This time gap has been associated with:
 - For SPH simulations, there is a relation with the SPH particle size
 - For Fluent (CFD) simulations, it could be related with missing 3D effects.
- Computational effort: because the synthetic pressures correspond to an analytical expression, the cost of obtaining these pressures is almost negligible. On the other hand, CFD or SPH are very costly making these approaches not yet affordable in current aircraft industry environment.

From the three numerical approaches, the synthetic pressures have been selected for aircraft design and certification because it is the methodology that provides the best level of accuracy and (once obtained the coefficients of the analytical expression) the lower computer cost.

The limitations of SMAES test results used to derive the synthetic pressures (i.e. results for rigid flat plates of X~1.0 m; at constant vertical speed and at constant pitch in each run etc.) have to be extended to complete aircraft geometry (X > 1.0 m), effect of flexibility, effect of curvature, variable vertical speed and variable pitch.

2.4 Structural response to a ditching excitation

Figure 10 shows the deformation exhibited by the bottom part of the fuselage of a medium transport aircraft explicit FEM model once subjected to the synthetic ditching pressures.

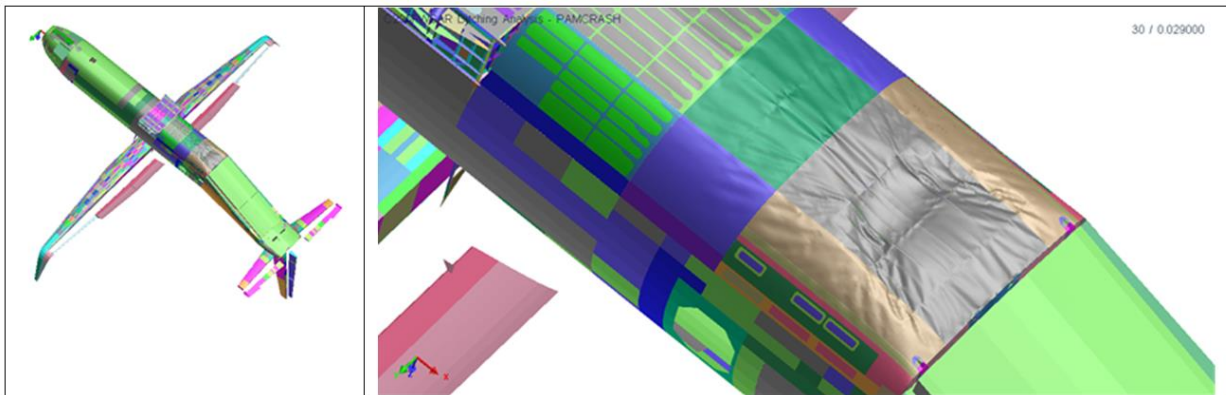


Figure 10. Left: aircraft structural deformation due to ditching pressures.. Right: local detail zoom.

In addition to analyse the FEM model deformation, it is possible to integrate the loads in riveted-joint sections for subsequent checkstress analyses. As an example, figure 11 shows a schema of the fuselage bottom part (longitudinal lines are stringers, transversal lines are frames) with a normalized map of loads (in KN) of riveted-joint section loads to be transmitted to the checkstress offices.

| | | | | | | | | | | | | | | | |
|------|------|----|------|----|--------|----|--------|----|--------|----|------|----|------|------|------|
| 41 | 50 | 39 | 58 | 68 | 42 | 54 | 49 | 41 | 41 | 55 | 30 | | | | |
| | | 22 | 36 | | | | 56 | 51 | | | 35 | | | | |
| | | 24 | 28 | | | | 49 | 48 | | 24 | 29 | 49 | 34 | 51 | |
| | | 37 | 37 | | | | 43 | 45 | | 43 | 46 | | | | |
| | | 30 | 40 | | | | 39 | 47 | | 25 | 22 | | | | |
| 29 | 44 | 24 | 30 | 83 | 100 | 93 | 31 | 37 | 75 | 70 | 31 | 29 | 62 | 53 | 65 |
| | | 18 | 32 | | | | 45 | 51 | | 24 | 23 | | | | |
| | | 18 | 31 | | | | 28 | 21 | | 17 | 17 | | | | |
| | | 34 | 50 | | | | 43 | 52 | | 35 | 26 | | | | |
| | | 27 | 35 | | | | 39 | 38 | | 18 | 36 | | | | |
| | | 43 | 40 | | | | 52 | 57 | | 39 | 40 | | | | |
| FR22 | FR23 | | FR24 | | FR24.1 | | FR24.2 | | FR24.3 | | FR25 | | FR26 | FR27 | FR28 |

Figure 11. Example of integrated loads in bottom fuselage riveted-joints sections (in kN, normalized)

3. Ditching Floatation Phase

3.1 General considerations in the aircraft ditching floatation phase

The floatation phase begins once the aircraft comes to rest after the impact and sliding phases reach an end. The aircraft lies on water at a particular time-varying trim during the floatation stage, influenced by leakage, wing position and environmental conditions. The evacuation of occupants is performed at this phase.

The floatation phase is of concern to the Airworthiness Authorities. EASA CS 25.801 on ditching states that it is required to demonstrate that a safe occupants evacuation is attainable given a favourable attitude and aircraft floatation time under probable water conditions. Numerical methods are employed to provide quantitative answers to this problem. The following lines provide a description of the numerical approach used by the Industry to tackle aircraft floatation problems, along with the assumptions and methodology involved. Results for a military transport aircraft are discussed.

The evacuation of occupants is not the only relevant event occurring during the floatation stage. The gaps located between the aircraft doors and fuselage airframe comprise a set of sources enabling water ingress into the aircraft internal cavity, altogether with the collection of orifices given by the different valves and tubes placed at different aircraft locations. Furthermore, water leakage can be exacerbated during the floatation phase if the aircraft results damaged during the impact and sliding phases, since damage acts as an important source of water ingress. Leakage affects total aircraft floatation time in a negative way.

In addition, the aircraft equilibrium position, defined by the attitude itself, at each instant of time along the floatation phase is not only influenced by the aircraft design and geometric shape, but also by the amount of water leaked and the respective orientation of such volume within the aircraft.

Civil airworthiness requirements should consider aircraft floatation after a ditching event only in calm water conditions. On the other hand, military aircraft customers often require considering the presence of waves in aircraft floatation. Leakage and the aircraft trim will be affected by the environmental conditions or sea state. These constitute the local characteristics which define a given waterline, typically provided in terms of wave amplitude and frequency values. The Douglas sea scale is an internationally-used indicator which relates the wave height and swell with a specific degree of roughness, provided in terms of a scalar value ranging from zero to nine. Figure 12 shows the wave height in Douglas Sea Scale and a sketch with the leakage rate considering dynamic water line.

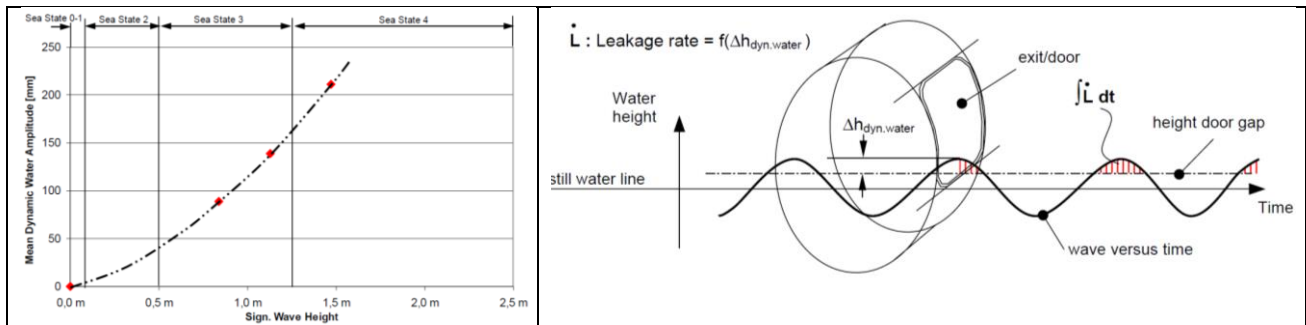


Figure 12. Douglas Sea Scale (left). Leakage rate considering dynamic water line – Transversal waves (right)

3.2 Aircraft floatation phase solver

The model-independent, in-house, numerical software tool suite developed with the purpose of simulating floatation scenarios considers not only primary contributions such as leakage, equilibrium position determination and occupants evacuation, but also takes into account the motion of fuel within the aircraft tanks and the environmental conditions. Figure 13 shows a flowchart of this solver.

The software workflow begins with the interpretation of the floatation model, which comprises the description of leakage sources, and the aircraft cavities involved in buoyancy and leakage computations. The latter constitutes a collection of equally-sided volumetric prismatic elements which adapts to the aircraft overall geometric shape.

The equilibrium position is determined assuming quasi-static conditions at each instant of time in consideration. A dedicated non-linear solver computes the required aircraft attitude which satisfies the Archimedes principle, so that the summation of vertical forces and longitudinal and lateral moments is zero, and consequently performs stability analyses to gather the stable attitude solutions only. This step takes into consideration the position of the aircraft overall center of gravity (influenced by the empty aircraft center of gravity value, leaked water position and fuel position) and center of buoyancy.

As a result, the stable static equilibrium position determination corresponds to the computation of the stable trim characteristics which ensure that the aircraft center of gravity is vertically aligned to the center of buoyancy with respect to axes attached to the waterline. Low-wing aircraft typically present pitch-up and levelled-wing attitude at the beginning of the floatation phase, whilst high-wing aircraft pitch-up and rolled trim characteristics.

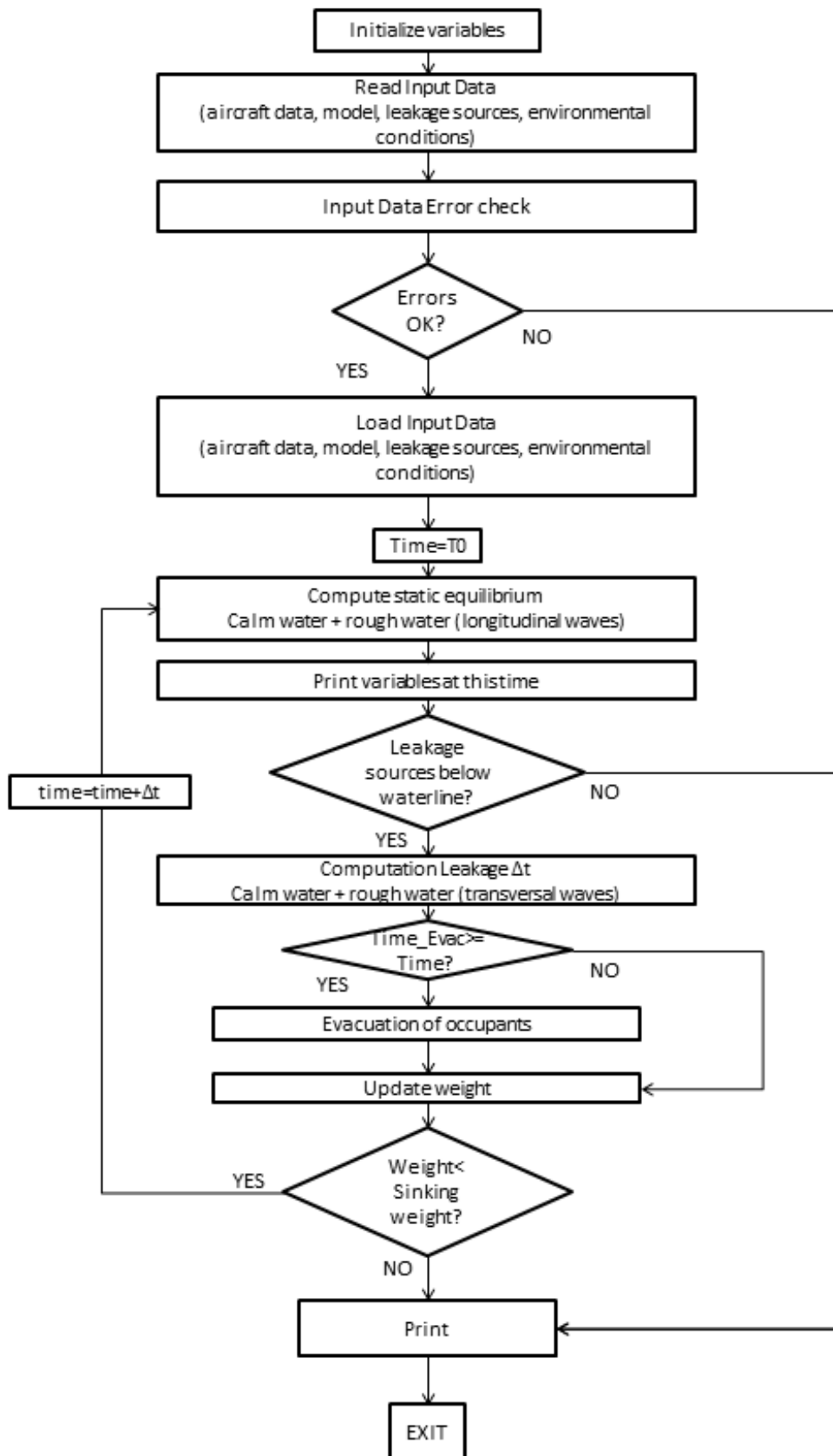


Figure 13. Flootation Solver Flowchart

Water leakage is computed next, applying Torricelli principle:

$$\dot{Q} = \eta A \sqrt{2gh} = \frac{\Delta V_{\text{leak}}}{\Delta t} \quad (2)$$

Where η denotes the discharge coefficient (influenced by the orifice geometric shape), A is the leakage source effective area, g is the Earth gravity acceleration and h is the effective height of water above a given leakage source. The effective height is computed by comparing the position of a given leakage source with respect to two water levels, generally, the external water plane and the internal water plane reached when water accumulates within a particular aircraft cavity. The aircraft door gaps are modelled as a combination of interconnected individual orifices.

The evacuation of occupants is also performed during the computation loop to update the overall aircraft weight, also dependent on the amount of water leaked.

Environmental conditions are taken into account to model two primary contributions occurring in rough water scenarios: **dynamic waterline (transversal waves)** and **leaked water sloshing (longitudinal waves)**. The dynamic waterline is modelled by computing the uncoupled vertical motion of the aircraft with respect to the wave itself in the following way:

$$\sum F_z = m\ddot{z} = \rho_{\text{water}} g V_{\text{submerged}}(z) - mg \quad (3)$$

The dynamic waterline or equivalent wave affecting the aircraft floatation characteristics is computed after subtracting the wave model to the resulting z . This equivalent wave is used to compute leakage, which can considerably increase with respect to calm water scenarios.

The vertical motion or heave of the aircraft can be decoupled from the general equations of motion governing the dynamics of a floating body, when the waves characteristic wavelength is considerably larger than the typical body reference length, i.e.: aircraft length. Sea State 4 conditions, corresponding to 2.5 meter-high waves, are an example of typical rough waterlines in which some military aircraft are required to be ditching-certified. These waves characteristic wavelengths span hundreds of meters, overcoming typical aircraft lengths.

Water sloshing consists in the motion followed by the leaked water within the aircraft internal cavity when the aircraft floats in rough water scenarios, affecting the position of the overall center of gravity. Longitudinal water sloshing is considered to be more influential than lateral sloshing, as there is less room for water to accommodate laterally within a given aircraft internal cavity. Water sloshing is modelled by modifying the position of the leaked water volume periodically.

The numerical software tool suite is validated through a number of test cases. Simplified scenarios where basic geometric shapes like cubes or cylinders with an associated leakage source float on water, restraining rotations and considering only the vertical motion, constitute a series of test cases whose physics can be described in terms of analytical expressions. The numerical solution reached by the in-house software tool, after reproducing these scenarios numerically, is compared to the analytical results. More complex problems like aircraft floating at a determined time-varying trim are not described by analytical expressions. To validate the numerical capability of the in-house tool, the numerical solutions reached with the latter are benchmarked to the numerical solution provided by third parties.

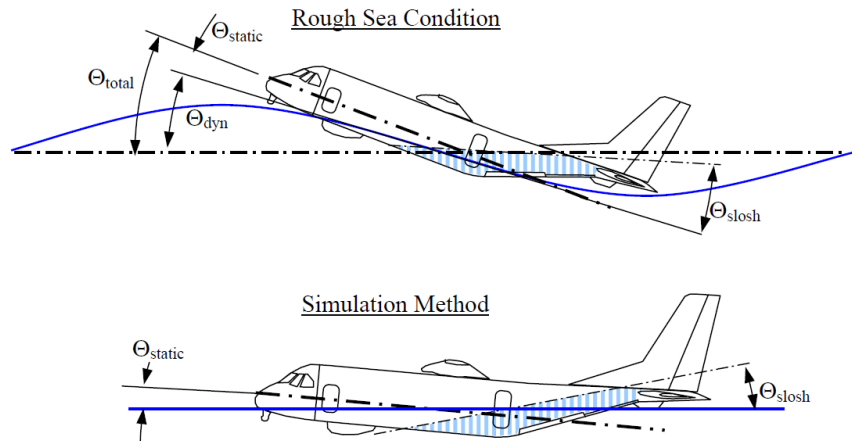


Figure 14. Consideration of internal flow sloshing (longitudinal waves) in aircraft floatation in rough sea condition

3.3 Aircraft floatation results

Figure 15 shows the trim angles evolution versus time of an undamaged high-wing military aircraft with critical mass state and center of gravity configuration when floating in calm water scenarios, and all doors distance to the external water plane (sill height) evolution. 42 occupants are assumed to be evacuated at a constant rate.

It is shown that the floatation time spans 931 seconds, and that the aircraft is completely evacuated after 399 seconds, leaving enough margin to perform a safe evacuation.

Furthermore, it is appreciated that the aircraft follows a pitch-up and roll to the right attitude during the floatation phase, being this trim evolution distinctive of high-wing aircraft. The doors located aft and rightwards are submerged from the beginning of the floatation phase, precluding evacuation. The hatch (door located at the top of the aircraft fuselage) stays above the external water line during the complete evacuation phase. Thus, it is required from the design and evacuation standpoint the presence of this kind of doors in high-wing aircraft to perform evacuation safely.

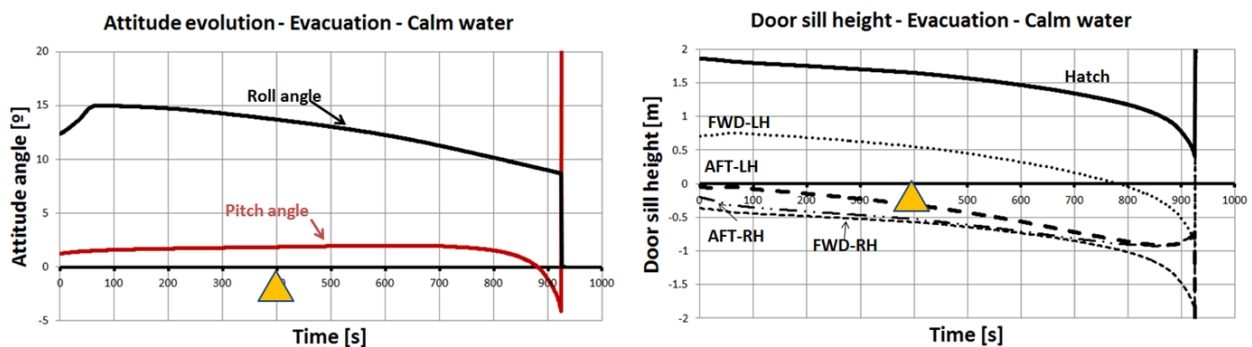


Figure 15. Floatation results: attitude (left) and door sill height evolution (right) – Evacuation – Calm water

The variation of the floatation time is also addressed when analysing the scenario where no occupants are evacuated. This configuration is critical in terms of floatation time since it reaches a minimum, whilst keeping the remaining aircraft model characteristics unchanged. Thus, evacuation acts as a weight relief process, enhancing the floatation capability of a given aircraft, increasing the floatation time (see Figure 16, left)

The environmental conditions also influence the floatation time. It is maximum in calm water scenarios and minimum when considering the full dynamics problem: dynamic waterline and sloshing in Sea State 4 conditions, since water leakage increases, as appreciated in Figure 16 (right).

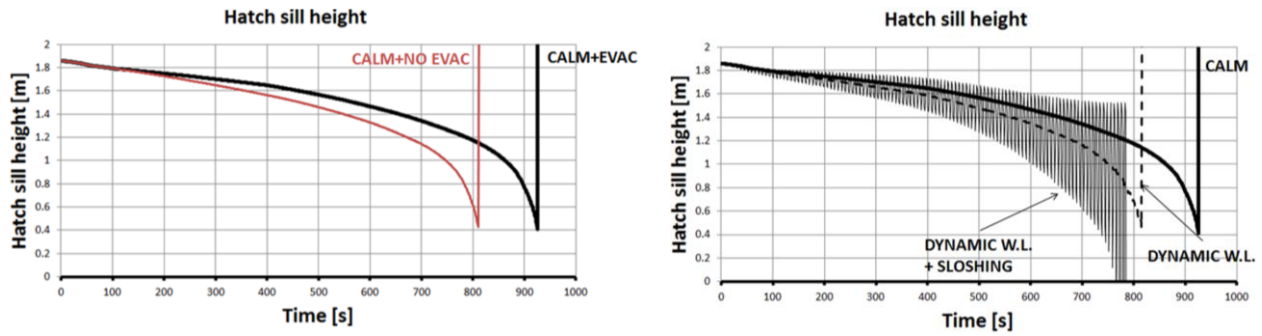


Figure 16: Hatch sill height evolution – Evacuation/No evacuation (left) – Calm water/Sea State 4 conditions (right)

Finally, figures 17 and 18 show respectively:

- Figure 17, the external floatation sequence with the relative position of the aircraft versus the sea.
- Figure 18, the internal floatation sequence with the level of internal amount of water.

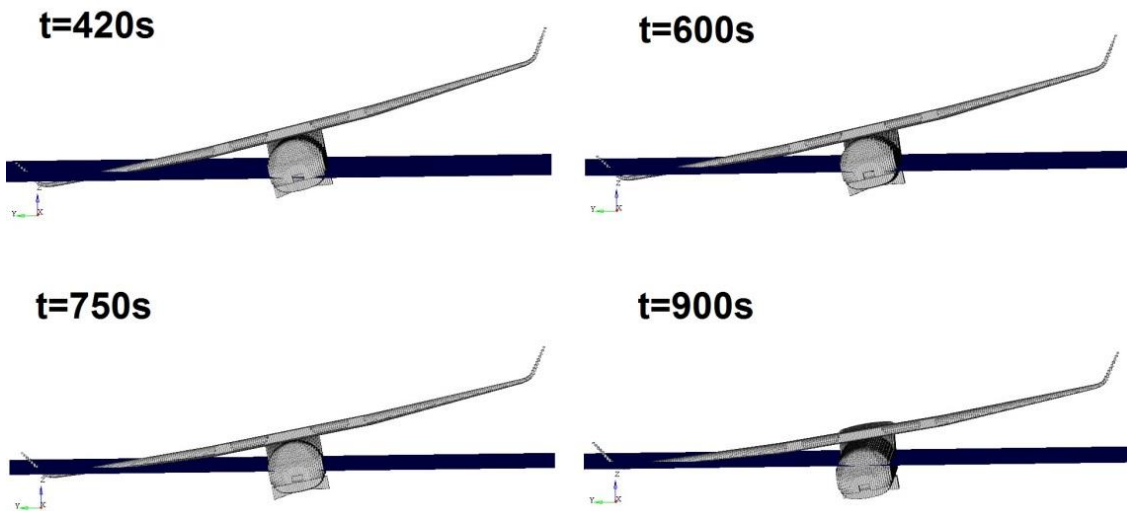


Figure 17: Aircraft floatation analysis results. Typical external sequence

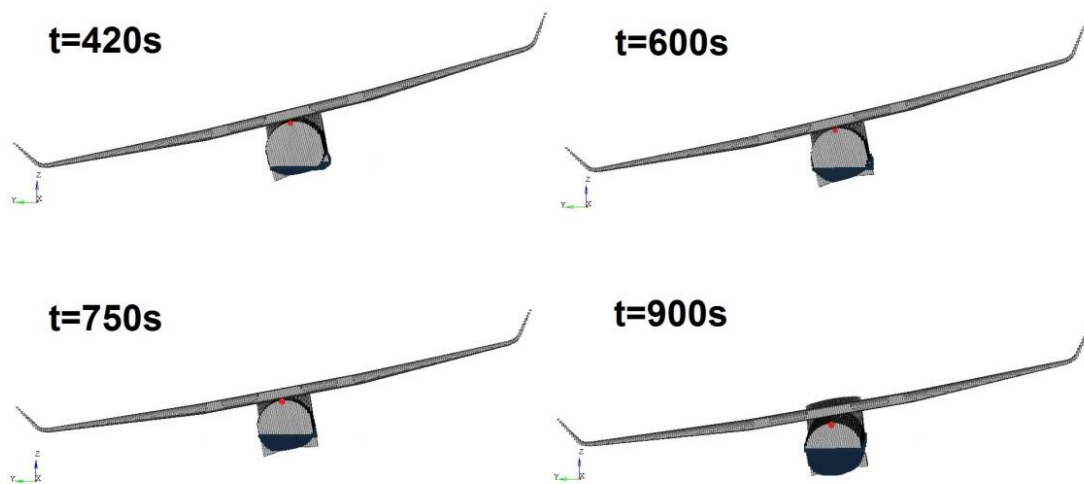


Figure 18: Aircraft floatation analysis results. Typical internal sequence

4. Conclusions

The paper has presented the work that the structural dynamics department of a manufacturing aircraft company has to perform for the design and certification of an aircraft from the ditching standpoint. The tasks of this department are concentrated in two of the four phases of ditching: impact phase and floatation phase.

Impact phase: the aircraft structure has to be modelled using explicit FEM technique with very fine mesh in the impact zone (under the fuselage). The excitation loads during a ditching scenario is a difficult aspect. This paper has presented a comparative analysis among three different numerical methodologies to simulate ditching loads: SPH, CFD and synthetic pressures (analytical expression that matches ditching test results). The three of them have been compared with ditching test results measured in the EU funded SMAES program. The comparison has concluded that the synthetic pressures is –currently- the most suitable approach to be considered in design and certification of a real aircraft. Aircraft structural response obtained by numerical simulations (using these models and excitation) provide evidence of structural integrity either directly or (like in the example of integrated loads in riveted joints) producing data for subsequent checkstress analysis.

Floatation phase: once the aircraft has reached a rest it is necessary to demonstrate enough buoyancy time to ensure safe evacuation of the aircraft. A floatation tool has been briefly presented in the paper that accounts for two “military” aspects not usually considered in civil certification: inertia relief due to servicemen evacuation and the effect of rough water with sea waves in the Douglas Scale 4 range.

Future activities in ditching research include extension of flat plate measurements to real aircraft geometries, to determine the “ballistic limit” of thin panels in ditching and further research of the behaviour of riveted-joint areas under ditching loads.

5. Acknowledgments

Part of the work leading to the results presented has received funding from the European Commission’s Seventh Framework Programme under grant agreement no FP7- 266172 and was performed within the project SMAES — SMart Aircraft in Emergency Situations.

References

- [1] Climent, H., Benitez, L., Rosich, F., Rueda, F. and Pentecote, N. “Aircraft Ditching Numerical Simulation,” 25th Congress of International Council of the Aeronautical Sciences ICAS 2006. Hamburg, Germany, 3-8 September 2006.
- [2] Siemann, M., Kohlgrueber, D., Benitez Montañés, L., and Climent, H. “Ditching Numerical Simulations: Recent Steps in Industrial Applications,” Proceedings of the Aerospace Structural Impacts Dynamics International Conference, Wichita, Kansas, 6-9 November 2012.
- [3] Climent, H., Viana, J.T., Benítez Montañés, L., Pérez Muñoz, J.D. and Kamoulakos, A. “Advanced Simulation (using SPH) of Bird Splitting, Ditching Loads and Fuel Sloshing,” Proceedings of the ESI Global Forum 2014. Paris (France), 21-22 May 2014.
- [4] Climent, H., Pastor, G., Viana, J.T., Benítez, L. and Iafrazi, A. “Experimental Ditching Loads”. Proceedings of the International Forum of Aeroelasticity and Structural Dynamics IFASD 2015. Saint Petersburg, Russia, 28 June -2 July 2015. (ISBN 9781510821828).
- [5] Viana, J.T., Romera, J., Pastor, G., Benítez, L., Climent, H. and Siemann, M.H. “Numerical Simulation of Ditching Dynamic Loads”. Proceedings of the International Forum of Aeroelasticity and Structural Dynamics IFASD 2015. Saint Petersburg, Russia, 28 June -2 July 2015. (ISBN 9781510821828).
- [6] Romera, J. “Structural Loads in a ditching Situation”. Master Thesis. Escuela Técnica Superior de Ingeniería Aeronáutica y del Espacio. Universidad Politécnica de Madrid. July-2015.
- [7] Climent, H. “Aerospace Impacts Technology. An Industrial Perspective,” Keynote Lecture at the Aerospace Structural Impact Dynamics International Conference ASIDIC, Seville (Spain), 17, 18 November 2015.

- [8] Pastor, G., Viana, J.T., Benitez, I., Climent, H. and Iafrati, A. "Recent Progress in Experimental Ditching Loads". Proceedings of the Aerospace Structural Impact Dynamics International Conference ASIDIC, Seville (Spain), 17, 18 November 2015.
- [9] Viana, J.T., Romera, J. Pastor, G. Benitez, L. and Climent, H. "Structural Response to Ditching Loads," Proceedings of the Aerospace Structural Impact Dynamics International Conference ASIDIC, Seville (Spain), 17, 18 November 2015.
- [10] Climent, H, Viana, J.T. and Pastor, G. "Preliminary Analytical Expression for Aircraft Ditching Loads," Presented at the Airbus Group Workshop on Aeroelasticity, Structural Dynamics and Loads, Toulouse (FR), June 7-8 2016.
- [11] Luis Valle, A.M. "Effect of Structural Flexibility on Ditching Loads". BSc Thesis. Bachelor in Aerospace Engineering. Universidad Carlos III de Madrid. June 2017.
- [12] Climent, H, Pastor, G. and Viana, J.T. "Experimental Ditching Loads on Aeronautical Flexible Structures," Proceedings of the International Forum of Aeroelasticity and Structural Dynamics IFASD 2017. Lake Como, Italy, 26-28 June 2017.
- [13] Viana, J.T., Pastor, G. and Climent, H. "Flexible Structures Response to Ditching Loads," Proceedings of the Aerospace Structural Impact Dynamics International Conference ASIDIC, Kansas City (USA), 17-19 October 2017.
- [14] Mateos Llorente, A. "Effect of Structural Flexibility on Ditching Loads". BSc Thesis. Bachelor in Aerospace Engineering. Universidad Carlos III de Madrid. 9-June-2018.
- [15] Pérez Heredia, E. "Prediction of Aircraft Ditching Loads with Computer-Aided Simulations". Master Thesis. Escuela Técnica Superior de Ingeniería Aeronáutica y del Espacio. Universidad Politécnica de Madrid. 13-Sep-2018.
- [16] Iafrati, A. and Grizzi, S. "Cavitation and ventilation modalities during ditching", Phys. Fluids 31, 052101 (2019); <https://doi.org/10.1063/1.5092559>
- [17] Iafrati, A. "Experimental investigation of the water entry of a rectangular plate at high horizontal velocity" Journal Fluid Mechanics, Vol. 799, pp. 637-672, 2016. Doi: 10.1017/jfm.2016.374
- [18] Iafrati, A., Grizzi, S., Benitez-Montañes, L. and Siemann, M. "High-speed ditching of a flat plate: Experimental data and uncertainty assessment" Journal of Fluids and Structures, Vol. 55, pp. 501-525, 2015. Doi: 10.1016/j.jfluidstructs.2015.03.019 "
- [19] Virtual Performance Solution/PAM-CRASH Manual. ESI-Group Trademark. 2010.